Pakistan Veterinary Journal

ISSN: 0253-8318 (PRINT), 2074-7764 (ONLINE)
DOI: 10.29261/pakvetj/2026.001

RESEARCH ARTICLE

# Transcriptomics Reveal the Potential Antiviral Mechanism of Dihydromyricetin in the Brains of Jiangkou Radish Piglets Challenged with Pseudorabies Virus

Wei Sun[1*], Fengming Zhou[1*], Yu Fan[1], Nannan Zhu, Shengqing Deng[1], Qingyan Wang[2], Samuel Kumi Okyere[3] and Shanshan Liu[1$]

[1]Tongren Polytechnic University, Bijiang District, Tongren City, Guizhou, 554300, China; [2]Wenzhou Vocational College of Science Technology, Wenzhou 325006, China; [3]Department of Pharmaceutical Sciences, School of Medicine, Wayne State University, Detroit, USA
*Corresponding author: huojianbaifenbai@163.com

ARTICLE HISTORY (25-559)

Received: June 14, 2025
Revised: August 16, 2025
Accepted: August 19, 2025
Published online: January 12, 2026

**Key words:**
Dihydromyricetin
Pseudorabies virus
Transcriptomics
Wnt/β-catenin signaling pathway

**ABSTRACT**

Pseudorabies virus (PRV) is an economically damaging swine herpesvirus infecting diverse hosts. The Wnt/β-catenin pathway is crucial for many viruses, including PRV. This study investigated the antiviral potential and mechanisms of dihydromyricetin (DHM), a compound with known antiviral activity, against PRV infection in the brains of Jiangkou Radish Piglets. PRV-infected piglets were treated with DHM. Brain analysis showed DHM reduced PRV-induced pathological damage, specifically mitigating mitochondrial and synaptic injury. Transcriptome sequencing identified 600 differentially expressed genes (DEGs; 328 upregulated, 272 downregulated) in DHM-treated vs. untreated infected brains. Gene Ontology (GO) enrichment linked these DEGs to glutathione metabolism, L-glutamate transport, synapse function, and neurotransmitter processing, suggesting that DHM may combats oxidative stress and regulates neuronal communication. Kyoto Encyclopedia of Genes and Genomes (KEGG) analysis categorized DEGs into 30 pathways. Key modulated pathways included glutathione metabolism, the Wnt signaling pathway, and the synaptic vesicle cycle, indicating potential antiviral mechanisms. Validation confirmed significant expression changes in key Wnt pathway genes (β-catenin, GSK3β, c-myc), supporting the transcriptome results. The study demonstrates that DHM may exerts antiviral effects against neurotropic PRV in piglet brains by alleviating neuronal damage and modulating critical biological processes and signaling pathways, particularly such as the Wnt/β-catenin pathway, however, there is the need for further validation studiesoffering insights for PRV therapy.

**To Cite This Article:** Sun W, Zhou F, Fan Y, Zhu N, Deng S, Wang Q, Okyere SK and Liu S, 2026. Transcriptomics reveal the potential antiviral mechanism of dihydromyricetin in the brains of jiangkou radish piglets challenged with pseudorabies virus. Pak Vet J. http://dx.doi.org/10.29261/pakvetj/2026.001

## INTRODUCTION

Pseudorabies, also referred to as Aujeszky's disease, is a condition brought about that is caused by the pseudorabies virus (PRV) (which is also known as Aujeszky's disease virus or Suid herpesvirus-1). This disease has resulted in significant economic damage to pig farming operations in various countries (Su *et al*., 2024). PRV is a sophisticated DNA virus that is a member of the Herpesviridae family and the Alphaherpesvirinae subfamily. Pigs are recognized as the sole natural reservoirs for PRV. Infections in young piglets and mature pigs with virulent strains of PRV can lead to sudden death and severe clinical manifestations such as neurological symptoms(Hanson, 1954; Sehl and Teifke, 2020). Beyond pigs, a variety of other animals such as cattle, sheep, cats, dogs, raccoons, minks, and skunks are also susceptible to PRV infection. Moreover, there have been occasional reports of potential human infections with PRV with symptoms such as conjunctivitis, dermatitis, fatal encephalitis, and significant disorders of the central nervous system(Yang *et al*., 2019). These reports indicate that PRV continues to pose a considerable risk to public health. Therefore, it is imperative to enhance the study of the pathogenic mechanisms behind PRV infection.

The Brain tissue is characterized by high oxygen consumption and robust energy metabolism (Hubbard *et al*., 2024). The release of neurotransmitters and synaptic

plasticity both rely on mitochondrial metabolism. Thus, mitochondrial dysfunction may result in neuronal damage, thereby affecting various body's behaviors controlled by the brain (Halliwell, 2010). PRV replicates in neurons around infected tissues and migrates to the central nervous system through the peripheral nervous system, causing immune responses in the central nervous system and pathological damage (Hsu *et al.*, 2024).

Dihydromyricetin (DHM), a dihydroflavonol compound abundantly present in Ampelopsis species of the grape family, possesses multiple pharmacological activities (Li *et al*., 2017 and Zhao *et al.,* 2018 ). Studies have shown that DHM exhibits strong DPPH scavenging activity, hinders the generation of reactive oxygen species (ROS), diminishes oxidative stress, and demonstrates excellent antioxidant, anti-inflammatory, antibacterial, antiviral, and immunomodulatory properties (Liu, 2019). The antiviral activity of DHM has gained significant attention over the recent years (Xin *et al*., 2015). Our previous research indicated that DHM exerts potent antiviral effects by inhibiting viral replication, limiting viral activity, and modulating excessive inflammatory immune responses. In addition, preliminary findings from our laboratory suggest that DHM can neutralize PRV and inhibit its invasion, thereby exerting antiviral effects (Sun *et al*., 2022).

Jiangkou Radish Pig, a precious local genetic resource breed in China, is an endemic and distinctive local variety originating from Tongren City, Guizhou Province. Unfortunately, this unique breed faces the threat of PRV. However, the existing research reports on the interaction between the Jiangkou Radish Pig and PRV are scarce, emphasizing the urgent need for further studies to gain a deeper understanding of the risks posed by PRV and to devise effective mitigation strategies. DHM has shown promising antiviral activity over recent years. However, the specific mechanisms by which DHM exerts its antiviral effects remain unknown. To clarify the gene expression changes of DHM during PRV infection, we utilized RNA-seq technology to investigate the gene expression profiles changes associated with DHM antiviral activity. This study will provide valuable information for the research on pathogenesis and serve as a reference for discovering potential therapeutic interventions targeting PRV infections.

## MATERIALS AND METHODS

**Reagents:** Antibodies against GSK3β, β-catenin, c-myc, and β-actin were sourced from Abcam and Beijing Biosynthesis Biotechnology. Two-month-old Jiangkou Radish piglets came from a Jiangkou County farm. The PRV-HLJ strain (MK080279.1) was provided by the Harbin Veterinary Research Institute. PCR reagents (2×SYBR Green Mastermix, RR820A; reverse transcription kit, RR047A) were from TAKARA. The RNA extraction kit (B518621) was from Sangon Biotech. Dihydromyricetin (DHM) was extracted from *Ampelopsis grossedentata* plant per prior methods.

**Experimental design:** Twenty-four weaned Jiangkou Radish piglets (2 months old, ~10 kg) were randomly allocated to 4 groups (n=6 piglets/group, individually housed with ad libitum access to food/water for 28 days). The dosage of DHM was determined according to the study by previous study (Hou *et al*., 2014). Control: Pigs were given Basal diet only, DHM Group (A): Pigs were given Basal diet + 400 mg/kg DHM, PRV+DHM Group (B): Basal diet + 400 mg/kg DHM; injected with PRV (2mL, $1\times10^3$ $TCID_{50}$/100μL) on day 21, PRV Group (C): Basal diet only; injected with PRV (as Group B) on day 21. On day 28, piglets were euthanized by electrical stunning followed by exsanguination. Brain tissue was rapidly collected for analysis.

**Histopathology:** Fresh brain tissue was fixed in 4% formaldehyde (>24h), processed (dehydration, paraffin embedding), sectioned (4-5μM), mounted, deparaffinized, stained with Hematoxylin and Eosin (H.E.), and examined using digital microscopy.

**Ultrastructural morphology**: Fresh brain tissue (1 $mm^3$ pieces) was fixed in 2.5% glutaraldehyde (2h) and post-fixed in 1% osmium tetroxide. After the tissue was dehydrated in graded acetone, infiltrated with resin, and sectioned (100 nm). The sectioned samples were stained with uranyl acetate and lead citrate and examined by transmission electron microscopy.

**Transcriptome analysis:** Total RNA was extracted from brain samples. Libraries were sequenced on an Illumina Novaseq™ 6000. Raw reads were quality-controlled (Cutadapt: remove adapters/polyG/polyA; FastQC: Q20/Q30) and aligned to a reference genome (HISat2). Gene expression was quantified as FPKM. Principal Component Analysis (PCA, R "gmodels") assessed sample relationships. Differential gene expression (DEGs) between groups was identified using DESeq2 (|Fold Change| ≥2, FDR <0.05). Biological significance of DEGs was explored via Gene Ontology (GO) and KEGG pathway enrichment analyses (DAVID platform, P<0.05).

**qRT-PCR:** Total RNA was extracted from brain samples ("Animal Total RNA Isolation Kit"), assessed for integrity (agarose gel) and quantity/quality (NanoDrop-2000). cDNA was synthesized ("PrimeScript RT reagent Kit"). qRT-PCR used SYBR Green I on a LightCycler 96, with specific primers (designed via Oligo.7, synthesized by Sangon Biotech; see Table 1). Relative mRNA expression was calculated using the 2-ΔΔCt method, normalized to β-actin.

**Table 1:** qRT-PCR Primer Information

| Gene Name | Primer Name | Sequence | Product Size(bp) |
|---|---|---|---|
| GSK3β | GSK3β F | 5′-AGATCACTGTAACATAGTCCGATTGC-3′ | 85 |
| | GSK3β R | 5′-CAGCACCAGATTAAGATAGACCTCATC-3′ | |
| β-catenin | β-catenin F | 5′-GCTCTTGTGCGTACTGTCCTTC-3′ | 92 |
| | β-catenin R | 5′-TGGTGTCGGCTGGTCAGATG-3′ | |
| c-myc | c-myc F | 5′-TCTCCTCCGCCGAGTCCTC-3′ | 109 |
| | c-myc R | 5′-TCCTCATCCTCTTGTTCTTCCTCAG-3′ | |
| β-actin | β-actin-F | 5′-TCGCCGACAGGATGCAGAAG-3′ | 113 |
| | β-actin-R | 5′-CAGGATGGAGCCGCCGATC-3′ | |

**Western blotting:** Total protein was extracted from brain tissue ("Tissue Protein Extraction Kit") and quantified (Bradford method). Proteins were separated by 10% SDS-PAGE, transferred to PVDF membranes, blocked (5% skim milk), and probed overnight at 4°C with primary antibodies: GSK3β (1:1000), β-catenin (1:800), c-myc

(1:500), β-actin (1:1200). Membranes were washed (PBST), incubated with HRP-conjugated secondary antibody (1h), washed again, and visualized (ECL). Band intensity was quantified (ImageJ2x), normalized to β-actin.

**Immunohistochemistry (IHC):** Brain tissue was fixed (4% paraformaldehyde), processed, paraffin-embedded, and sectioned (5μM). Sections were deparaffinized, underwent antigen retrieval, and were blocked. Primary antibodies (GSK3β 1:500, β-catenin 1:300, c-myc 1:200) were applied overnight. After washing, biotinylated secondary antibodies were applied (37°C, 20 min), followed by DAB staining, hematoxylin counterstaining, bluing (ammonia water), and microscopic examination.

**Statistical analysis:** Data are presented as mean ± SD. Differences between groups were analyzed using one-way ANOVA (SPSS v22.0). Significance levels were set at $P<0.05$ and $P<0.01$. Graphs were generated using GraphPad Prism 6.0.

## RESULTS

**DHM treatment protects against PRV-induced pathological brain damage:** DHM treatment protected the brain from pathological damage associated with PRV infection (Fig. 1). The brain tissues in the control group (Fig. 1-Con) and Group A (Fig. 1-A) had intact and visible meninges, neurons glial cells, and had nerve fibers completely present within the cerebral cortex. The neuronal cells in the brain tissues of Group B (Fig. 1-B) and C (Fig. 1-C) showed a higher number of oligodendrocytes (green circle and red circles respectively). Furthermore, as shown in Table 2, the severity of the lesions was ranked from severe to mild as follows: Group C (1.67) > Group B (0.67) = Group A (0.67) > Control group.

**Table 2:** Intergroup scoring table for increased number of oligodendrocytes surrounding neurons in brain tissue.

| Group | Number of samples | Cumulative score | Average score | Judgment criteria |
|---|---|---|---|---|
| Control | 3 | 0 | 0 | The international guidelines for terminology and diagnostic criteria of pathological changes in rats and mice (INHAND). China Agriculture Press. November 2019. |
| A | 3 | 0 | 0 | |
| B | 3 | 2 | 0.67 | |
| C | 3 | 5 | 1.67 | |

**DHM protects the mitochondrial and synaptic from damage caused by PRV:** The results from the electron microscopic analysis revealed notable differences in the ultra-structural features of brain mitochondria and synapses among the control group, the DHM-treated group, the PRV-infected group, and the DHM and PRV treatment group. As shown in Fig. 2, the control group showed intact mitochondrial membranes with well-preserved cristae structures (Fig. 2-Con, black ellipses) and an intact synaptic structure (Fig. 2-Con, black circles) with an indicative of normal neuronal connectivity. In contrast, the PRV-infected group showed mitochondrial membrane damage and blurred cristae structures (Fig. 2-C, red ellipses) as well as marked alterations in the synaptic (Fig. 2-C, red circles) ultra-structures. However, when DHM was administered concurrently with PRV infection, we observed that the mitochondrial ultra-structure remained surprisingly intact and well-preserved with visible cristae structures even though the synaptic structures (Fig. 2-B, red circle) still exhibited signs of damage.

**Correlation and DEG in brain tissue after treatment:** High-throughput sequencing revealed that 915,535,874 raw reads were generated in Con, DHM, DHM+PRV, and PRV samples. After filtering out reads with adapter sequences, a total of 887,852,416 clear and unrepeated reads were retained. The percentage of reads with a quality score exceeding 30 (Q30) exceeded 98.16% across all samples (Table 3).

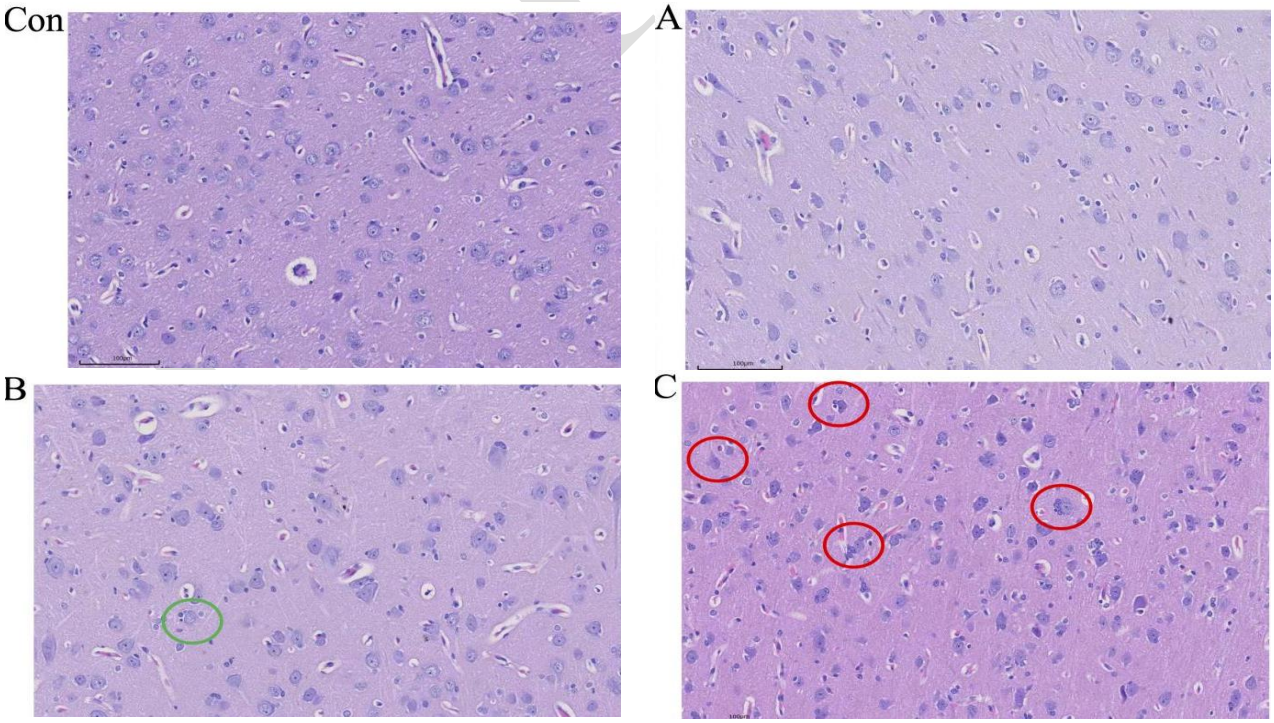


**Fig. 1:** The pathological observation on Brain(Bar=100 μm).The red and green circles represent the increased number of oligodendrocytes surrounding neuronal cells. (Con) Control group; (A Group A; (B) Group B; (C) Group C.

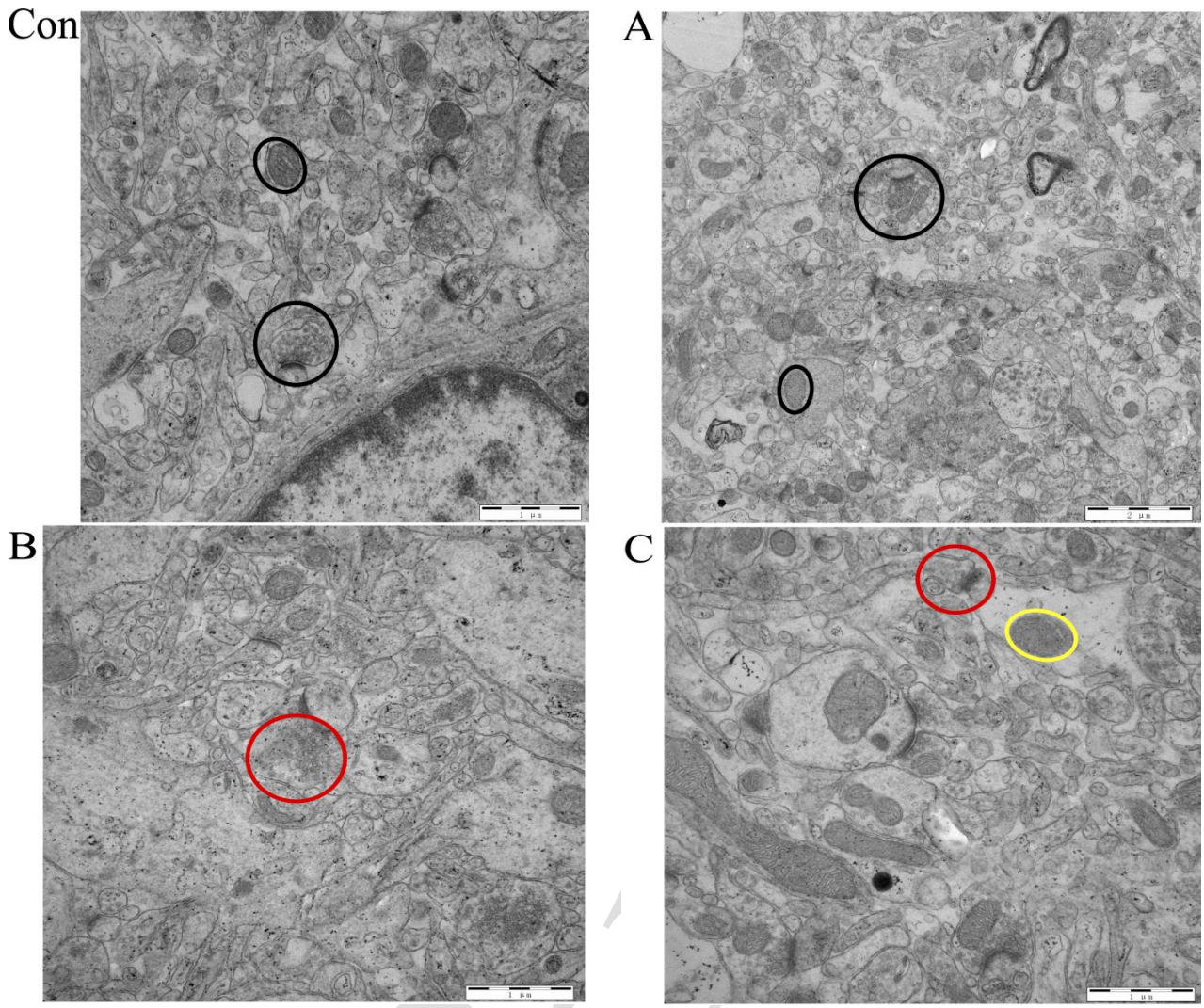


**Fig. 2:** Effect of DHM on the ultrastructure of brain tissue (Bar=1 μm). Circles represent synapses, and ellipses represent mitochondria. Black circles and ellipses indicate normal structures, while red and yellow represent damaged synapses and mitochondria, respectively. (Con) Control group; (A) Group A; (B) Group B; (C) Group C.

**Table 3:** Preliminary Data Processing and Quality Control Statistics

| Groups | Raw Reads | Clean Reads | Raw Bases (Gb) | Clean Bases (Gb) | Effective Rate (%) | Q30 (%) |
|---|---|---|---|---|---|---|
| A1 | 4.17E+07 | 4.01E+07 | 6.26 | 6.01 | 96.04 | 98.29 |
| A2 | 4.20E+07 | 4.05E+07 | 6.30 | 6.07 | 96.30 | 98.30 |
| A3 | 4.17E+07 | 4.01E+07 | 6.26 | 6.02 | 96.11 | 98.23 |
| B1 | 4.04E+07 | 3.89E+07 | 6.06 | 5.83 | 96.29 | 98.30 |
| B2 | 4.09E+07 | 3.93E+07 | 6.14 | 5.90 | 96.20 | 98.25 |
| B3 | 4.01E+07 | 3.85E+07 | 6.02 | 5.78 | 96.08 | 98.17 |
| C1 | 4.05E+07 | 3.90E+07 | 6.08 | 5.84 | 96.12 | 98.20 |
| C2 | 4.07E+07 | 3.92E+07 | 6.11 | 5.87 | 96.15 | 98.22 |
| C3 | 4.36E+07 | 4.20E+07 | 6.53 | 6.30 | 96.41 | 98.70 |
| CONTROL1 | 4.08E+07 | 3.91E+07 | 6.12 | 5.86 | 95.86 | 98.16 |
| CONTROL2 | 4.10E+07 | 3.94E+07 | 6.15 | 5.91 | 96.11 | 98.22 |
| CONTROL3 | 4.05E+07 | 3.88E+07 | 6.07 | 5.82 | 95.81 | 98.27 |

As illustrated in Fig. 3, the Pearson correlation coefficient and Principal Component Analysis (PCA) were employed to assess the distinctions between the DHM treatment group, the DHM+PRV group, the PRV-challenged group, and the mock group. Fig. 3A depicts that the Pearson correlation coefficient results indicated a robust correlation among duplicates within each treatment group, with correlation values surpassing 0.845. Likewise, the PCA analysis unveiled distinct distributional differences between each group (Fig. 3B). In addition, we employed the log10(FPKM+1) method to conduct pairwise comparisons among various treatment groups, aiming to explore the variations in DEGs (Fig. 4). The results revealed a total of 600 DEGs, comprising 328 up-regulated genes and 272 down-regulated genes. Furthermore, the heatmap displayed all DEGs between the two groups. The results indicate that the control group and the treatment group exhibited similar expression patterns.

**GO analysis of DEGs:** The GO enrichment analysis results in Fig. 5 revealed that a total of 88 significantly enriched GO terms were found in different treatment groups, including 25 biological process (BP), 15 cell component (CC), and 10 molecular function (MF). Among them, 25 major subcategories of BP mainly involve glutathione metabolic, axon guidance, regulation of DNA template transcription, RNA polymerase II-mediated transcription regulation, G protein-coupled receptor signaling pathways, signal transduction, glutathione metabolism, L-glutamate transport, and L-glutamate transport across the plasma membrane. The 15 major subcategories of CC mainly consist of membranes, cytoplasm, nuclei, and synapses. Finally, the 10 major

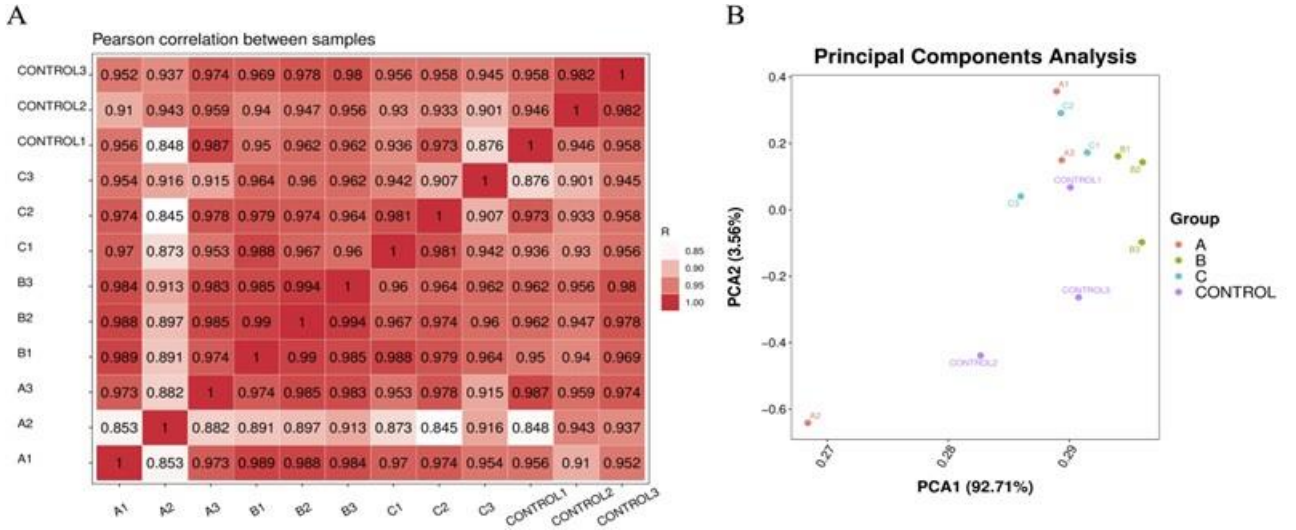


**Fig. 3:** Sample correlation analysis. A correlation coefcient heatmap for all control groups, revealing highly consistent measurements within groups, R2≥0.845; (B)A PCA plot was used to cluster samples, revealing good repeatability. Each point represents one sample, green and red circles respectively correspond to all samples, and percentages denote contribution ratios.

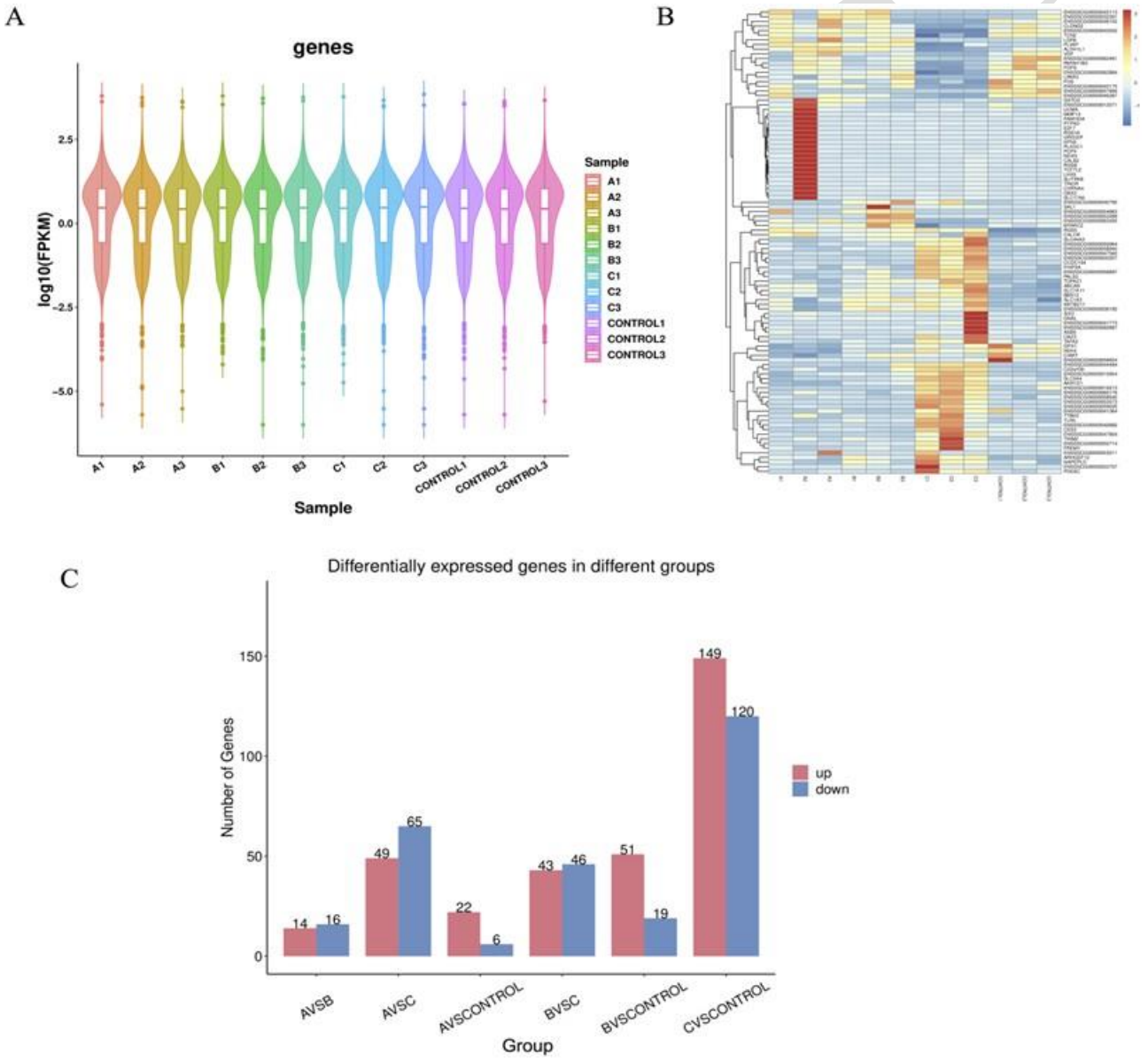


**Fig. 4:** Analyses of the transcriptomic profiles of all groups. (A) Quantification of the mRNA expression levels indicated by log10 (FPKM+1), contrasting control piglets versus the treatment group; (B) Clustered heatmap of the distinct expression patterns of mRNAs across paired samples between groups; (C) The total number of up-regulated and down-regulated DEGs between different groups.

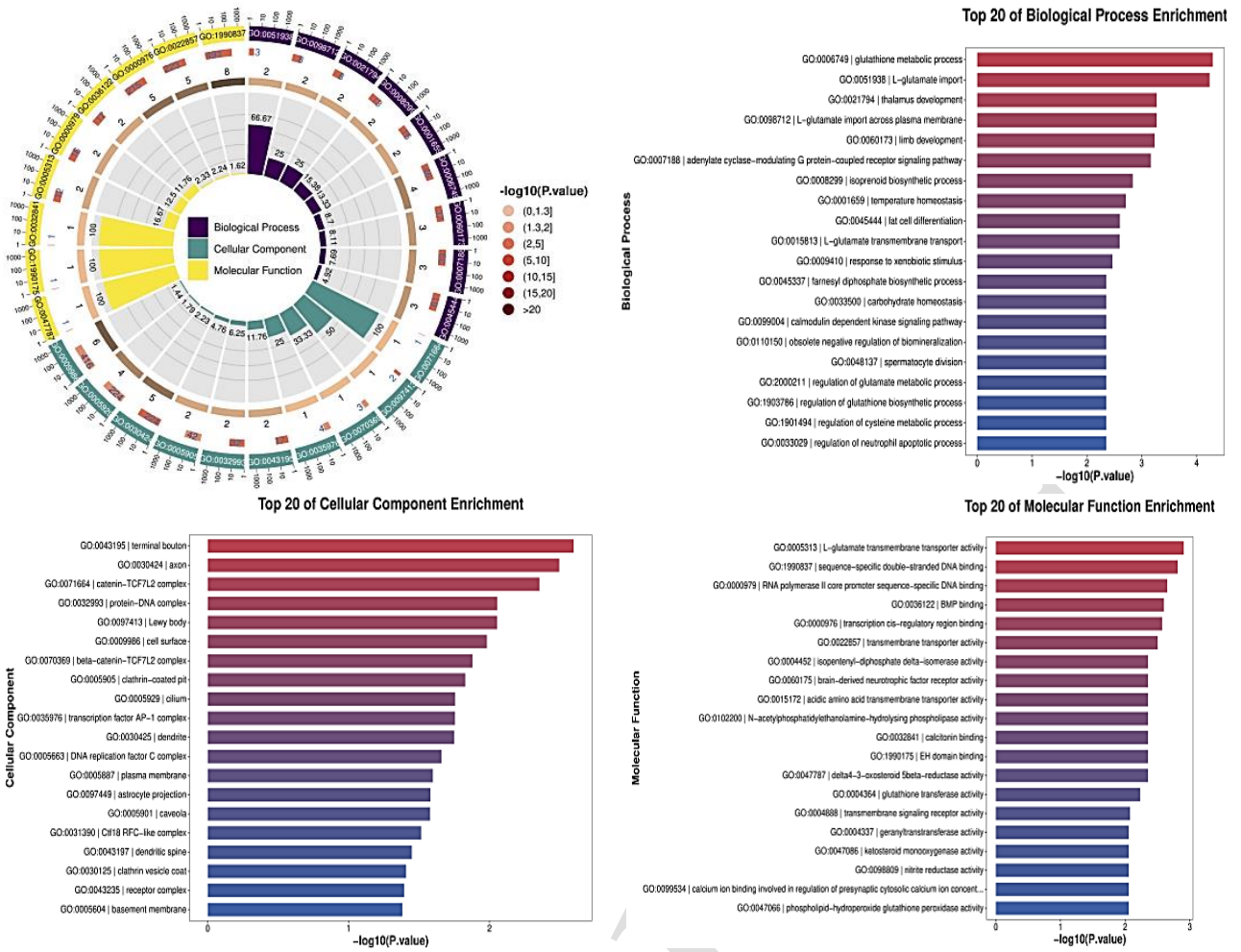


**Fig. 5:** GO enrichment analysis. Loop diagram of GO bar plot. Top 20 of Biological Process Enrichment, (C) Cellular Component Enrichment, (D)Molecular Function Enrichment.

subcategories of MF were mainly related to DNA binding and nucleotide binding. These results indicate that the DEGs in different groups are related to the functions of the brain in glutathione metabolism, L-glutamate transport, synapse, and L-glutamate transmembrane transporter activity. The findings suggest that DHM may regulate key cellular processes related to oxidative stress defense (glutathione metabolism), neurotransmitter processing (L-glutamate transport and transmembrane transporter activity), and neuronal communication (synapse). The alterations in these functional pathways may contribute to the antiviral effect of DHM against PRV by disrupting viral replication or enhancing the resistance of host cells to infection.

**KEGG pathway of DEGs:** In total, 600 DEGs were identified across all groups, which were classified into 30 KEGG pathways (Fig. 6). To be exact, each of the following categories had 5 KEGG pathways within them: Cellular Processes, Environmental Information Processing, Genetic Information Processing, Human Diseases, Metabolism, and Organismal Systems. The most represented pathways were Terpenoid backbone biosynthesisssc, Drug metabolism- cytochrome P450, Glutathione metabolisms, Wnt signaling pathway, and Synaptic vesicle cycle calculated by P value. In addition, it also involved neuroactive ligand-receptor interaction and Cholinergic synapse. In summary, these findings suggest that DHM may exert its antiviral effect against PRV by modulating multiple crucial biological processes and signaling pathways. However, further validation is required to confirm these observations.

**Validation of key genes in Wnt signaling pathway:** Given the crucial role of the Wnt signaling pathway in tissue homeostasis and disease onset, regulating cell proliferation, differentiation, and migration, we selected three key genes within this pathway for further validation at both the gene and protein levels. The results revealed a profound and statistically significant up-regulation ($P<0.01$) of the β-catenin gene in the DHM, DHM+PRV, and PRV infection groups compared to the control group. Intriguingly, the β-catenin expression level in the DHM+PRV treatment group was notably lower ($P<0.01$) than that in the DHM and PRV mono-therapy group, suggesting that DHM could prevent the upregulation of β-catenin induced by PRV. Conversely, the DHM+PRV group alone significantly up-regulated ($P<0.01$) the GSK3β and c-myc gene compared to the control, whereas PRV caused a marked down-regulation ($P<0.01$ or 0.05) of GSK3β and c-myc compared to the control. This finding indicated that DHM might exert an inhibitory effect on PRV through modulation of GSK3β and c-myc. These findings were consistent with the western blot (Fig. 7) and immunohistochemical analyses (Fig. 8), results. The

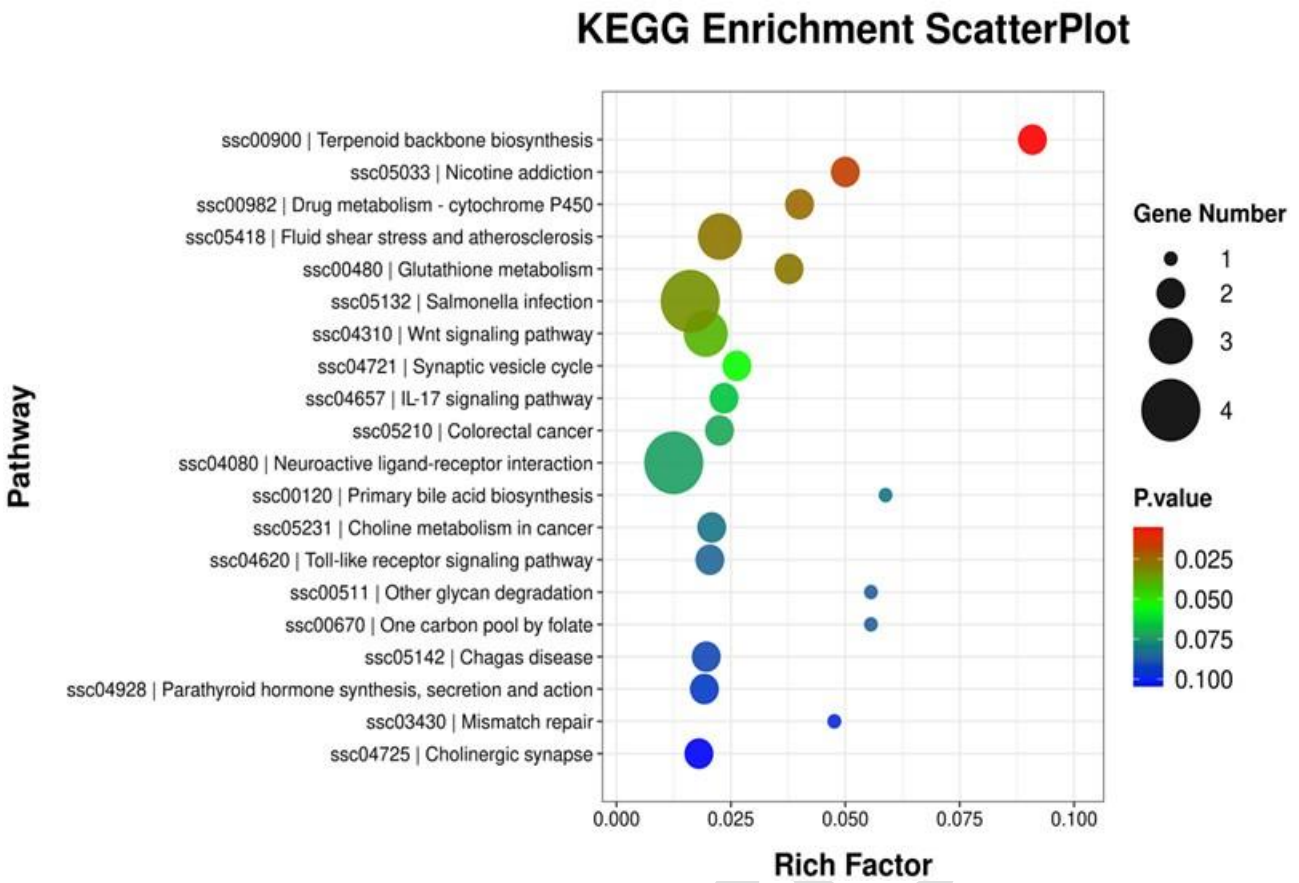


**Fig. 6:** Bubble diagram of KEGG pathway analysis of differential expression genes. screened with |Log2 (Fold change) > 1.5 and *p*-value adjusted <0.05. The rich factor represents the relative abundance of such genes within a given pathway, compared to its total gene count.

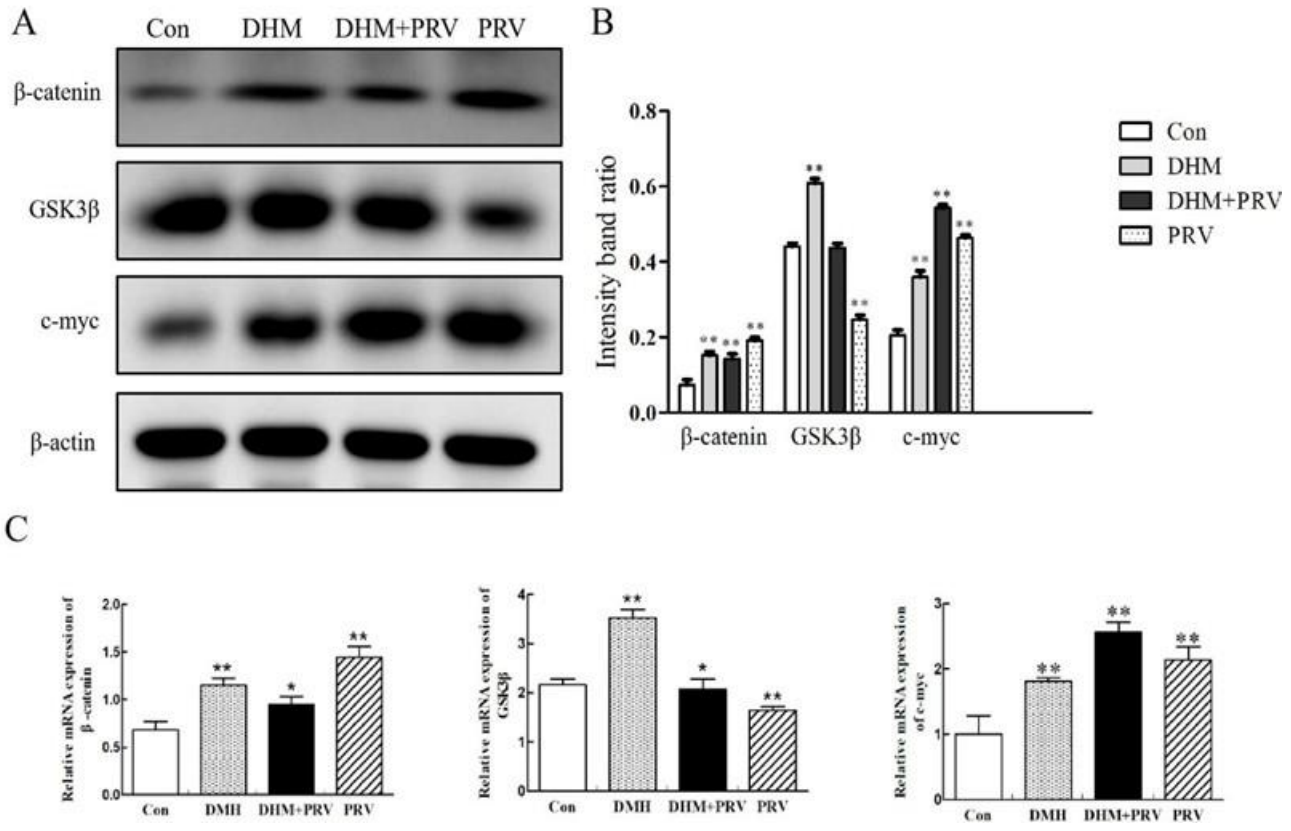


**Fig. 7:** Expression Levels of Factors Associated with the Wnt Signaling Pathway among all groups. (A)The protein expression levels of β-catenin, GSK3β and c-myc, as determined by Western blotting analysis in different treatment groups (Con, DHM, DHM+PRV, and PRV); (B) Quantification of protein expression as the ratio of target protein to β-actin; (C) Relative mRNA expression levels of β-catenin, GSK3β, and c-myc. Data are presented as mean ± SEM. Significant differences between groups are indicated by * (P<0.05) and ** (P<0.01).

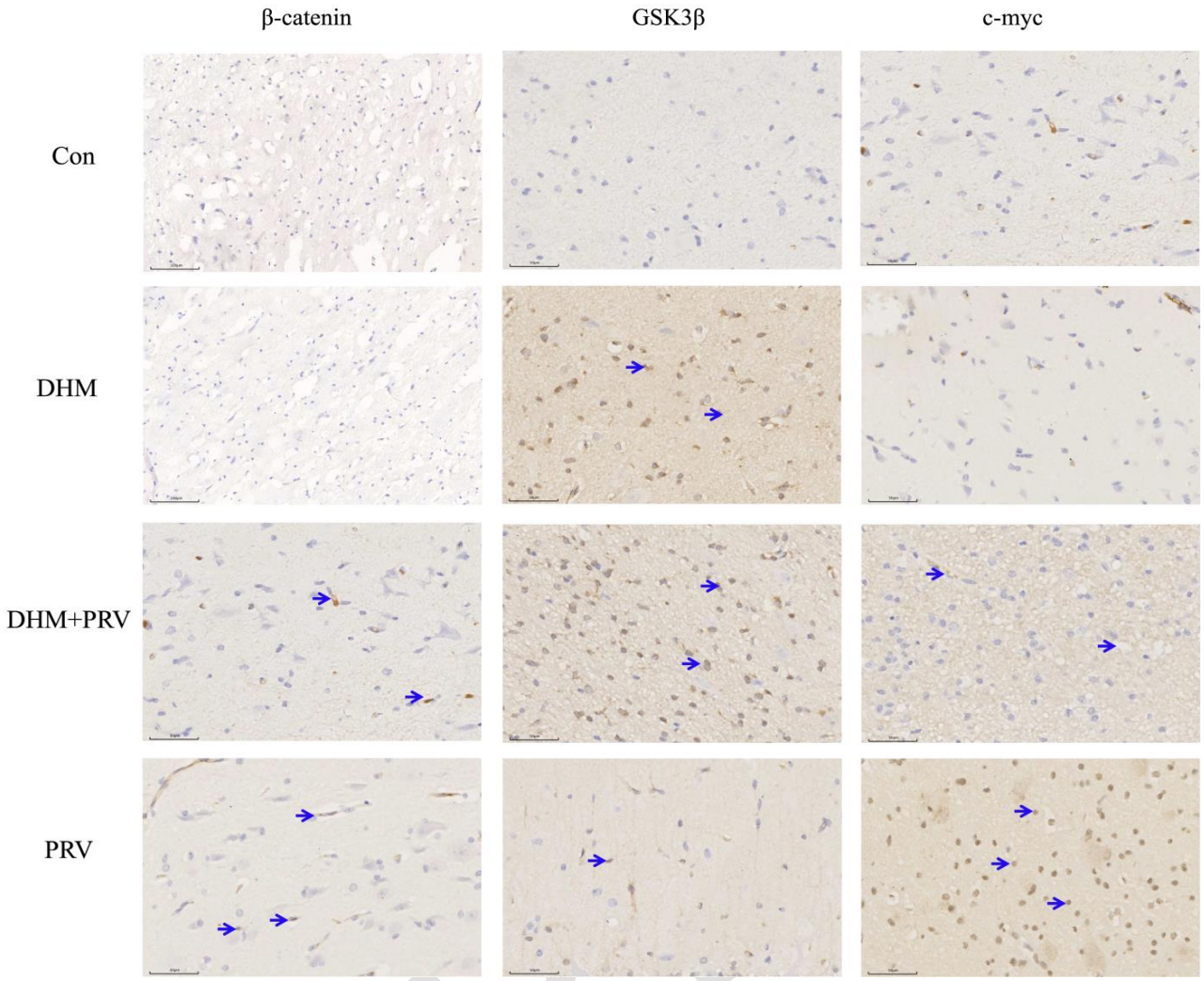


**Fig 8:** Immunohistochemical Analysis protein expression in brain tissue following different treatments. Blue arrows indicate positively β-catenin, GSK3β, and c-myc stained cells.

congruence between gene and protein expression levels with sequencing outcomes underscores reliability and high confidence in the transcriptome sequencing results obtained in this study. However, this finding requires further in-depth study to validate this claim.

## DISCUSSION

In latter part of 2011, a novel strain of PRV surfaced in pig farms across China, despite the widespread administration of the Bartha-K61 vaccine. These variant strains have proven to be resistant to the traditional attenuated vaccine (Bartha-K61 strain), leading to insufficient protection and considerable economic losses for the pig industry(Jiang *et al*., 2024). Currently, therapeutic options for pseudorabies are scarce, and vaccination remains the primary method for preventing and controlling PRV, including attenuated and inactivated vaccines(Liu *et al*., 2022). Vaccination represents the paramount approach for preventing the extensive dissemination of PRV. Despite this, live vaccines may enhance the diversity of viral strains and expedite the risk of strain mutation. Inactivated vaccines also possess certain limitations, including having diminished capacity to elicit natural immunity, ability to extended duration of viral shedding, and induce severe immune-related side effects. Numerous studies have emphasized the widespread application of natural compounds in antiviral research due to their extensive bio-activity and abundant sources. DHM exhibits anti-inflammatory, antibacterial, and antitumor properties, offering significant potential for clinical applications(Jingyao *et al*., 2018). For example, DHM was reported to reduce the activation of the NLRP3 inflammasome and the lipopolysaccharide (LPS)-induced TLR4/NF-kB signaling pathway(Wei *et al*., 2022b). DHM has emerged as a potential therapeutic candidate for SARS-CoV-2 infections(Xiao *et al*., 2021). Furthermore, studies have shown that DHM possesses antiviral properties that inhibit the replication of the African swine fever virus (Chen *et al*., 2023).

In this study, we found that the dose of 400 mg/kg DHM did not cause the pathological change on the oligodendrocytes in the brain tissue of Jiangkou radish pigs. This results was consistent to the study of Matouk *et al*. (Matouk *et al*., 2024) which reported that DHM (at a dose of 400 mg/kg) attenuated the renal injury induced by Gentamicin. However, DHM effectively prevented the pathological change on the oligodendrocytes after PRV challenge. The results from the Electron microscopic ultrastructure revealed that DHM can effectively prevent mitochondrial damage but had limited ability to repair synaptic damage. This result indicated that DHM has the

potential to prevent the detrimental effects of PRV on mitochondrial structure. A study by Yuan *et al*.(Yuan *et al*., 2025) who reported that DHM could ameliorate mitochondrial structural damage in chicken. Nonetheless, the persistence of synaptic injury highlights the importance of further research to comprehensively understand the mechanisms that underlie DHM's protective effects and its limitations in preserving neuronal communication amidst viral infections.

The GO and KEGG enrichment analysis conducted in this study revealed that DHM may modulate crucial cellular processes associated with oxidative stress defense (glutathione metabolism), neurotransmitter processing (L-glutamate transport and transmembrane transporter activity), and neuronal communication (synapse) and pathways including terpenoid backbone biosynthes, drug metabolism- cytochrome P450 and Wnt signaling pathway cycle. These alterations in functional pathways may potentially contribute to the antiviral effect of DHM against PRV. Oxidative stress caused by increased levels of ROS is considered a major factor in various viral infections (Zimmerman, 1960). As a highly oxygen-consuming organ, the brain has weak antioxidant capacity and is prone to oxidative stress injury. With the occurrence of oxidative stress injury, intracellular antioxidant enzymes are excessively consumed, and their activity is inhibited, resulting in an imbalance between oxidation and antioxidation. The continuously accumulated ROS causes peroxidation of proteins and lipids and DNA damage, which induces the loss of neurons and synapses(Jamjoom *et al*., 2021). PRV has been reported by many studies to induce oxidative stress in tissues(Huan *et al*., 2025; Sun *et al*., 2023). Thus the association of DHM with the antioxidant system indicate that DHM may reduce oxidative stress associated with PRV infection just as reported in a study that reported that DHM could reduce oxidative stress through activation the SIRT3 pathway in pigs (Wei *et al*., 2022a).

Viral proliferation is intricately linked to the cellular processes of the host, with β-catenin, a central component of the Wnt/β-catenin signaling pathway, playing a crucial role in viral infections(Willert and Nusse, 1998). β-catenin interacts with IRF3, enhancing the expression of IFN-β, thereby modulating innate immune responses. Furthermore, TCF/β-catenin complexes bind to the promoter region of IFN-β, thereby inducing its production. Notably,You *et al*. (You *et al*., 2020) identified β-catenin as a fundamental component in cGAS/STING signaling-mediated IFN-I transcription, suggesting that Wnt/β-catenin pathway activation can hinders viral growth by modulating immune responses. Conversely, numerous viruses have developed strategies to inhibit the Wnt/β-catenin signaling pathway. For example, infection with bovine parainfluenza virus type 3 triggers the breakdown of β-catenin by increasing the expression of Gsk3β (Du *et al*., 2020). Similarly, porcine circovirus-like virus and Newcastle disease virus down-regulate β-catenin expression (Morla *et al*., 2019; Xuejiao *et al*., 2018). In addition, inhibition of GSK3β stimulates the Wnt/β-catenin signaling pathway and enhances the proliferation of PRV (Wang *et al*., 2022). The transcriptomics results in this study indicated that Wnt signaling is one of the critical signaling pathways. Furthermore, was discovered that DHM can suppress the expression of β-catenin while simultaneously enhancing the expression of c-myc and GSK3β, thereby activating the Wnt/β-catenin signaling pathway, which is consistent with findings from other research that revealed that DHM inhibited the protein expressions of β-catenin and GSK3β through the regulated extracellular-signal-regulated kinase (ERK)1/2 (Hsin *et al*., 2022; Zhang *et al*., 2014). However, this finding has not been validated in viral infections, thus we plan to investigate the effect of DHM on the Wnt/β-catenin signaling pathway after viral infection.

This comprehensive study, leveraging both transcriptomics pathway analysis, uncovers novel insights into how DHM might protect against PRV infection in Jiangkou Radish Pigs. The study provides foundational evidence that DHM can potentially protect tissues from PRV by inhibiting β-catenin expression and upregulating c-myc and GSK3β. However, there is the need for further in-depth investigations to fully validate the details of DHM's protective mechanisms observed in this study to make a solid conclusion and develop novel antiviral agents to safeguard neuronal communication during viral infections.

**Conclusions:** Given the antiviral properties of Dihydromyricetin (DHM), this study employs Jiangkou Radish Pigs as a model organism, utilizing histopathological analysis, electron microscopy, and transcriptomics techniques to screen for differentially expressed genes (DEGs). The findings reported that DHM has protective effect against PRV infection via modulating crucial cellular processes (associated with oxidative stress defense (glutathione metabolism), neurotransmitter processing (L-glutamate transport and transmembrane transporter activity), and neuronal communication (synapse)) and signaling pathways such as Terpenoid backbone biosynthesisssc, Drug metabolism- cytochrome P450, Glutathione metabolisms, Wnt signaling pathway, and Synaptic vesicle cycle. Thus, this study aims to provide a theoretical foundation for further in-depth study into the functional and mechanistic studies associated with DHM antiviral activity.

**Ethical statement:** This study received approval from the Animal Ethics Committee at Tongren Polytechnic University.

**Conflict of interest:** The authors of this study collectively affirm that there are no conflicts of interest present.

**Authors contribution:** Wei Sun contributed to the conceptualization, initial drafting of the manuscript and data analysis; Shanshan Liu performed qRT-PCR, Western blot analyses, and immunohistochemistry experiments; Wei Sun and Qingyan Wang undertook the responsibility of analyzing transcriptome data.; Fengming Zhou, Yu Fan, Nannan Zhu and Shengqing Deng were responsible for animal experiment management and sample collection; Samuel Kumi Okyere and Shanshan Liu provided supervisory guidance throughout the entire project.

**Funding statement:** This research was financially supported by Guizhou Provincial Basic Research Program

(Natural Science) (No.ZK[2024]664) and the Program of Cultivating High-Level Innovative Talents in Guizhou Province (No. 2022-(2020)-045).

**Data availability:** Data will be made available upon a reasonable request from the corresponding author. GSA data was stored at https://ngdc.cncb.ac.cn/ (with accession number PRJCA030908).

## REFERENCES


Chen Y, Song, ZB, Chang, H, *et al.,* 2023. Dihydromyricetin inhibits African swine fever virus replication by downregulating toll-like receptor 4-dependent pyroptosis in vitro. Vet Res 54(1):58.

Du X, He W, He H, *et al.,*2020. Beta-catenin inhibits bovine parainfluenza virus type 3 replication via innate immunity pathway. BMC Vet Res 16:72.

Halliwell B, 2010. Oxidative stress and neurodegeneration: where are we now? J Neurochem 97: 1634-1658.

Hanson R, 1954. The history of pseudorabies in the United States. J Am Vet Med A 124: 259-261.

Hsin MC, Hsiao YH, Chen PN., *et al*., 2022. Dihydromyricetin inhibited migration and invasion by reducing S100A4 expression through ERK1/2/β-catenin pathway in human cervical cancer cell lines. I J Mol Sci 23(23):15106.

Hsin MC, Hsiao YH, Chen PN., *et al*., 2022. Dihydromyricetin inhibited migration and invasion by reducing S100A4 expression through ERK1/2/β-catenin pathway in human cervical cancer cell lines. I J Mol Sci 23(23):p.15106.

Hsu Z, Engel E, Enquist L, *et al.,* 2024. Neuronal expression of herpes simplex virus-1 VP16 protein induces pseudorabies virus escape from silencing and reactivation. J Virol 98(7):e0056124.

Hubbard W, Velmurugan G and Sullivan P, 2024. The role of mitochondrial uncoupling in the regulation of mitostasis after traumatic brain injury. Neurochem Int 174:105680.

Huan C, Yang F, Zhang W, *et al*., 2025. Antiviral activity and antioxidant activity of Cistanche deserticola polysaccharides against pseudorabies viruses. Int J Biol Macromol 321:146326.

Hou X, Zhang J, Ahmad H, *et al*., 2014. Evaluation of antioxidant activities of ampelopsin and its protective effect in lipopolysaccharide-induced oxidative stress piglets. PLoS One 9(9):e108314.

Jamjoom A, Rhodes J, Andrews P, *et al.,* 2021. The synapse in traumatic brain injury. Brain 144: 18-31.

Jiang L, Cheng J , Pan H, Yang F, *et al.,* 2024. Analysis of the recombination and evolution of the new type mutant pseudorabies virus XJ5 in China. BMC Genomics 25:1-13.

Zhao JY, Chen J, Luo HQ, *et al.,* 2018. Recent Update on the Pharmacological Effects and Mechanisms of Dihydromyricetin. Front Pharmacol 25(9):1204.

Li H, Li Q, Liu Z, *et al.,* 2017. The Versatile Effects of Dihydromyricetin in Health. Evidence-based complementary and alternative medicine: eCAM 2017: 1053617.

Liu X, 2019. Dihydromyricetin: A review on identification and quantification methods, biological activities, chemical stability, metabolism and approaches to enhance its bioavailability. Trends Food Sci Tech 91: 586-597.

Liu Z, Kong Z, Chen M, and Shang Y, 2022. Design of live-attenuated animal vaccines based on pseudorabies virus platform. Animal Dis 2:11.

Matouk AI, Awad EM, Mousa AA, *et al.*, 2024. Dihydromyricetin protects against gentamicin-induced nephrotoxicity via upregulation of renal SIRT3 and PAX2. Life Sci 336:122318.

Morla S, Kumar A., and Kumar S, 2019. Newcastle disease virus mediated apoptosis and migration inhibition of human oral cancer cells: A probable role of β-catenin and matrix metalloproteinase-7. Sci Rep-UK 9:10882.

Nusse R, and Clevers H, 2017. Wnt/β-Catenin Signaling, Disease, and Emerging Therapeutic Modalities. Cell 169:985-999.

Sehl J and Teifke J, 2020. Comparative Pathology of Pseudorabies in Different Naturally and Experimentally Infected Species—A Review. Pathogens (Basel, Switzerland) 9:633.

Su B Yang G, and Wang B, 2024. Pseudorabies virus inhibits progesterone-induced inactivation of TRPML1 to facilitate viral entry. Plos Pathog 20:e1011956.

Sun W, Liu S, Lu A, *et al.,* 2022. In vitro anti-PRV activity of dihydromyricetin from Ampelopsis grossedentata. Nat Prod Res 36:4448-4451.

Sun W, Liu S, Yan Y, *et al*., 2023. Pseudorabies virus causes splenic injury via inducing oxidative stress and apoptosis related factors in mice. Sci Rep-UK 13(1):23011.

Wang C, Hu R, Duan L, *et al.,* 2022 The canonical Wnt/β-catenin signaling pathway facilitates pseudorabies virus proliferation and enhances virus-induced autophagy. Vet Microbiol 272:109502.

Wei Y, Hu Y, Qi K, *et al.,* 2022. Dihydromyricetin improves LPS-induced sickness and depressive-like behaviors in mice by inhibiting the TLR4/Akt/HIF1a/NLRP3 pathway. Behav Brain Res 423:113775.

Wei C, Chen X, Chen D, *et al*., 2022. Dihydromyricetin enhances intestinal antioxidant capacity of growing-finishing pigs by activating ERK/Nrf2/HO-1 signaling pathway. Antioxidants11(4):704.

Willert K, and Nusse R, 1998. Beta-catenin: a key mediator of Wnt signaling. Curr Opin Genet Dev 8:95-102.

Xiao T, Wei Y, Cui M, *et al.,* 2021. Effect of dihydromyricetin on SARS-CoV-2 viral replication and pulmonary inflammation and fibrosis. Phytomedicine 91:153704.

Xin M, Ma Y, Lin, W, *et al.,* 2015. Use of dihydromyricetin as antioxidant for polypropylene stabilization. J Therm Anal Calorim 120:1741-1747.

Xuejiao Z, Libin W, Shaoyang S, *et al.,* 2018. Porcine Circovirus-Like Virus P1 Inhibits Wnt Signaling Pathway in Vivo and in Vitro. Front Microbiol 9:390.

Yang H, Han H, Wang H, *et al.,* 2019. A Case of Human Viral Encephalitis Caused by Pseudorabies Virus Infection in China. Front Neurol 10:534.

Yuan L, Jiang X, Ren Y, *et al*., 2025. Dihydromyricetin ameliorates lipopolysaccharide–induced hepatic injury in chickens by activating the Nrf2/Keap1 pathway and regulating mitochondrial dynamics. Poultry Sci 104(5):105034.

You H, Lin Y, Lin F, *et al.,* 2020. β-Catenin Is Required for the cGAS/STING Signaling Pathway but Antagonized by the Herpes Simplex Virus 1 US3 Protein. J Virol 94:e01847-01819.

Zhang Q, Liu J, Liu B, *et al*., 2014. Dihydromyricetin promotes hepatocellular carcinoma regression via a p53 activation-dependent mechanism. Sci Rep-UK 4:4628.

Zimmerman H, 1960. American Association of Neuropathologists. J Neuropath Exp Neur 6.